Nanoscale Advances

ROYAL SOCIETY OF CHEMISTRY

COMMUNICATION

View Article Online
View Journal | View Issue



Cite this: *Nanoscale Adv.*, 2023, **5**, 1060

Received 29th September 2022
Accepted 14th January 2023

DOI: 10.1039/d2na00667g

rsc.li/nanoscale-advances

# Durability studies of underwater superoleophobic graphene oxide coated wire mesh†

Pichkari Saikiran, Mayuri Dhole and Nandini Bhandaru *

Due to the increased industrial oily wastewater, developing a successful oil/water separation mechanism is a ubiquitous challenge. As oil/water separation is an interfacial phenomenon, a straightforward way is to utilize the special wettability of novel materials towards oil and water. In this work, we intend to construct a durable membrane/mesh that can have a selective response towards oil and water based on the difference in surface tension. Graphene oxide (GO) is one such material that exhibits in-air hydrophilicity and underwater superoleophobicity. GO-coated wire meshes can act as membranes with excellent efficiency for oil/water separation, but they lack long-term durability for repeated use under different environments. We created GO*-coated wire meshes by dip coating multiple layers of GO with intermediate air plasma treatment. While the multiple steps of coating ensured complete coverage of the mesh with GO, plasma treatment improved the binding of the GO coating to the wire mesh. After coating five GO layers, the mesh is subjected to mild plasma treatment to improve the porosity. The GO*-coated mesh is extremely hydrophilic in air, and the underwater oil contact angles (CA) are ≥125° for different oils. To test the long-term durability, the GO*-coated mesh is continuously immersed underwater in acidic and basic media, and the underwater oil CA is measured at different immersion times. The initial durability results are very promising and show that the GO*-coated mesh retains a significant level of underwater oleophobicity even after 60 days of continuous immersion in water.



## 1. Introduction

Nanotechnology and its unique implications have evolved in nature in various forms. Many enchanting effects seen in nature, such as the water-repelling and self-cleaning properties of the lotus leaf, a water strider walking on water, the brilliant colors of a butterfly, or the super adhesion exhibited by spiders and geckos climbing on vertical surfaces, are essentially due to the presence of micro to nanoscale hierarchical structured surfaces with complex morphologies and chemical composition.[1] Several of these properties, if replicated into artificial materials, can lead to enormous benefits and multiple applications.[2–4] One such application garnering much attention and is the need of the hour is oil/water separation.[4,5] Oil/water separation techniques will have an immediate pragmatic contribution to fixing the obstacle of industrial oily wastewater and other pollution caused by oil.[6] With the fast development of our industries, oily wastewater discharge and oil spills have seriously polluted our environment. A swift environmental demand emphasizes the need for materials that can separate oil and water. The traditional separation processes used for separating oil and water require special equipment, consume high energy, and are expensive.[7] For example, mechanical devices such as oil skimmers,[8] agitated floatation cells,[9] and microwave heaters that use temperature change[10] all require high power and high pressures to aid in the separation. Other material absorption-based separation techniques include foams, sponges, or textiles,[11–13] but these materials have limitations such as poor selectivity towards oil and low efficiency, as well as their recycling being difficult and time-consuming.[7] To overcome these shortcomings, it is essential to design simple and economic approaches which are durable and can be implemented for large-scale oil/water separations.

For achieving oil/water separation, we need to target properties that are very different between oil and water. The surface tension of water is ~72.8 mJ $m^{-2}$, whereas, for most oils, surface tension is below 30 mJ $m^{-2}$. Thus, by creating porous membranes/meshes that have selective responses based on the surface tension of the liquid, one can achieve effective oil/water separation. Much research has been reported in this regard with the emergence of biomimetic water-repelling (superhydrophobic) and oil repelling (superoleophobic) surfaces inspired by the surface features of lotus leaves and springtails.[1,2] Novel materials with unique micro and nanoscale surface

*Department of Chemical Engineering, Birla Institute of Technology and Science Pilani, Hyderabad Campus, Pin – 500 078, Telangana, India. E-mail: nandini@hyderabad.bits-pilani.ac.in*

† Electronic supplementary information (ESI) available. See DOI: https://doi.org/10.1039/d2na00667g

structures have been ingeniously designed to achieve both superhydrophobic and superoleophobic properties.[14–16] But for the required oil/water separation, we need to fabricate materials that are either superhydrophobic/superoleophilic (high affinity towards oil) or superoleophobic/superhydrophilic (high affinity towards water).[4–7] In the first approach, the oil phase will spread quickly on the surface and penetrate it (in the case of a porous membrane), while the water phase will be repelled, resulting in oil/water separation.[17] However, as oil has a lower density than water, it is challenging to design an efficient separation technique for large-scale applications. Moreover, oil-removing membranes easily become fouled and clogged by the oil due to the oleophilic properties, reducing the separation efficiency.[4] The second approach of superoleophobic/superhydrophilic surfaces/membranes also has several limitations. Oil has a much lower surface tension than water, due to which a superhydrophilic surface exhibits superoleophilicity. In addition, making any surface oleophobic is not easy as there are no chemicals available that can directly achieve this property. Superoleophobicity has only been achieved by making specific micro and nanoscale structures with fluorinated polymers, which can be a complicated multi-step process.[4] However, the study of fish scales a decade ago showed that they are highly hydrophilic and, therefore, can exhibit superoleophobicity underwater and protect the fish from contagion by oil pollution in the sea.[18] This inspired the most effective and straightforward oil/water separation techniques reported till now based on membranes/meshes showing superhydrophilicity at the air/solid interface and superoleophobicity at the water/solid interface.

One of the first works on oil/water separation using a superhydrophilic and underwater superoleophobic mesh was reported by Xue *et al.* using PAM hydrogel-coated stainless steel meshes to separate water from oil/water mixtures with >99% efficiency.[19] However, hydrogels can swell quickly in water and have weak stability. Several other techniques and materials have been used since then for better functionalization of meshes. Coatings of organic materials such as polymers, block copolymers, polyelectrolytes, polymer blends, and polymer brushes have been extensively used to create hydrophilic water-selective meshes.[7,20–23] Copper (Cu), copper oxide, or copper hydroxide-based nanostructure-coated meshes have been the most widely reported inorganic functionalization techniques to obtain water-selective meshes.[3,24,25] Zhang *et al.* reported $Cu(OH)_2$ nanowire-haired copper mesh that can effectively separate oil/water mixtures and oil-in-water emulsions and provide long-term anti-fouling properties.[24] Apart from Cu, silica particles, carbon nanotubes, titanium dioxide nanoparticles, zeolites, and several other materials have also been used to functionalize metal meshes better. All the reported meshes with organic or inorganic materials have reasonable oil/water separation efficiency, but they either fail to give high filtrate flux or have poor chemical stability.[5,6] For better stability, direct etching of the metallic meshes using the laser ablation technique has been used for making more reusable meshes. But the method can be costly for large-scale oil/water separation. Recently, Lian *et al.* reported a nanosecond laser ablation technique to modify brass mesh, which they claim is low cost and more economical compared to previous methods.[26]

Of all the reported materials, graphene oxide (GO) coated membranes can be considered unique because of the layered nanostructure resembling that of fish scales or clamshells, abundant oxygen-containing functional groups, and excellent hydrophilicity, making them promising 2D meshes for oil/water separation.[27–31] Recently, simple GO coatings on brass or steel wire meshes have been reported with high separation efficiency. Dong *et al.* reported for the first time in 2014 that GO-coated stainless steel meshes have extraordinary hydrophilic and underwater superoleophobic properties and can be used for gravity-driven oil/water separation.[27] The GO-coated meshes showed very low oil-adhesion characteristics and separation efficiency above 90% with all types of oils. Liu *et al.* used $O_2$ plasma treatment after coating GO on the stainless-steel mesh to open clogged pores and change the pore diameter.[28] They achieved high separation efficiency even after 50 cycles of oil/water separation. Both works mention that finer meshes (300 or 400 mesh) with pore diameter of ~40 μm were best suited for oil/water separation. While GO coated meshes have been proven to be highly effective and promising for large-scale oil/water separation applications, to achieve a reasonable flux rate at low cost, we need to depend on a coarser mesh with larger pore size, and for long-term usage of these meshes, we need to have the excellent chemical stability of the GO coating.[31] Notably, for marine applications, the long-term effect of continuous immersion underwater on superoleophobicity must be checked.[32]

In this work, we report the preparation of a stable underwater superoleophobic mesh by dip-coating GO on a brass mesh. Air plasma treatment of the mesh was done before and after the GO coating steps. The initial plasma treatment of the bare mesh helped improve the adhesion between the GO and the metallic mesh. The dip-coating of GO was done multiple times to achieve complete coverage and a layered texture. After dip coating, the second plasma treatment resulted in the etching and opening of the fully obturate mesh pores. We also checked for the long-term durability of the GO coating on the wire mesh for the first time upon continuous immersion of the mesh in acidic, basic, and neutral media, mimicking the usual properties of industrial oily wastewater. We observed that the plasma-treated meshes remained superoleophobic underwater even after 60 days of immersion, while the untreated samples showed leaching of the GO coating within a couple of hours. We show that the plasma treatment steps significantly enhance the long-term stability and chemical durability of the GO coating on the wire mesh.

## 2. Materials and methods

### 2.1. Synthesis of GO

Graphite powder (~150 μm flakes, Sigma-Aldrich) was used as the raw material for the production of GO using a modified Hummers method.[33,34] During this synthesis protocol, 360 mL of sulfuric acid ($H_2SO_4$, SDFCL, 98% concentrated) and 40 mL of phosphoric acid ($H_3PO_4$, SD) (volume ratio 9 : 1) were stirred,

and 3.0 g of graphite flakes was added as depicted in step 1 of Fig. 1. In step 2, 18.0 g of potassium permanganate ($KMnO_4$, SRL) was slowly added under continuous stirring conditions. Stirring was done continuously for at least 20 hours, maintaining the temperature at 40 °C until the solution became dark green. The reaction mixture was then cooled to room temperature and then poured onto a mixture of 400 g of ice and 3 mL hydrogen peroxide ($H_2O_2$, Avra). During this step, ice was added to decrease its viscosity and avoid overheating, while $H_2O_2$ helps in the easy removal of metal salts like permanganate and manganese residuals from the mixture. Then, the mixture was centrifuged at 5000 rpm for 2 h (step 3, Fig. 1). After the decantation of the supernatant, the solid residuals were washed with 200 mL of hydrochloric acid (35% HCl, SD) and 200 mL of DI water in succession 3 times. Finally, the solids obtained after multiple rounds of washing were dried in an oven at 90 °C for 24 h to give 3.25 g of GO powder.

### 2.2. Characterisation of GO

To confirm the oxidation states achieved from the modified Hummers method, characterization was done for the synthesized powder using Fourier transform infrared (FTIR) spectroscopy (IRAffinity-1S in the range of 400–4000 $cm^{-1}$) and X-ray Photoelectron Spectroscopy (XPS, Thermo Fisher Scientific Pvt. Ltd, UK). FTIR determines the functional groups in the molecule, while XPS is a surface-sensitive quantitative spectroscopic technique that identifies the elements enveloping the surface. For better imaging of GO flakes, spin coating (Apex Instruments) was done to avoid agglomeration and the coffee stain effect as seen in the drop cast samples.[35] Scanning Electron Microscopy (FESEM, Model: Apreo LoVac), Atomic Force Microscopy (AFM, Agilent Technologies, USA), and Optical Microscopy (OM, Metavis) was used for imaging. Spin coating was done on a cleaned silicon wafer using a 0.25% dilute dispersion of GO in tetrahydrofuran (THF) at 1000 rpm. After spin coating, the coated samples were placed in an oven for 30 min at 60 °C and then imaged.

### 2.3. Methodology for coating of brass mesh with GO

Brass mesh (50 mesh) was used for the fabrication of the membrane. The brass mesh was cut into small pieces of 1.5 cm by 3.0 cm size and was cleaned by boiling and sonication in methanol and acetone. The cleaned pieces were exposed to air plasma treatment for 1 min (PDC-002, Harrick Plasma). The meshes were dip-coated with the dispersion of 0.25% GO in THF using a dip coater (Apex Instruments). After coating, the meshes were kept in an oven at 60 °C for 20 min. This step of dip coating and annealing was repeated 5 times to ensure proper coating of GO on the mesh. After coating, the meshes were again subjected to air plasma treatment for 1 min to unclog any closed pores. The mesh coated by this procedure, which includes plasma treatment, will be referred to as GO*-coated mesh. We also coated a few brass mesh pieces without any plasma treatment for comparison. These meshes will be referred to as GO-coated mesh. Optical Microscopy (OM, Metavis) was used to check the morphology of the GO*-coated mesh.

### 2.4. Measuring in-air and underwater contact angles

The in-air water CA ($\theta_w$) was measured by contact angle goniometry (Apex Instruments), and the underwater oil CA ($\theta$) was measured using a special setup with a J-shaped needle and a quartz water bath, such that oil can be easily dispensed on the mesh underwater. The different types of oils used were kerosene, toluene (HPLC, SRL), and edible oil (sunflower).

### 2.5. Durability

The long-term durability of GO*-coated brass meshes was studied by continuous immersion of the meshes in water (pH 7), acidic medium (pH 1.7), and basic medium (pH 12.9) for different durations up to 60 days. The acidic medium was prepared by adding 100 μL of sulphuric acid (98% concentrated) to 100 mL of DI water, and the basic medium was prepared by mixing 1 g of potassium hydroxide pellets in 100 mL of DI water. The meshes were taken out of the medium, air-dried, and

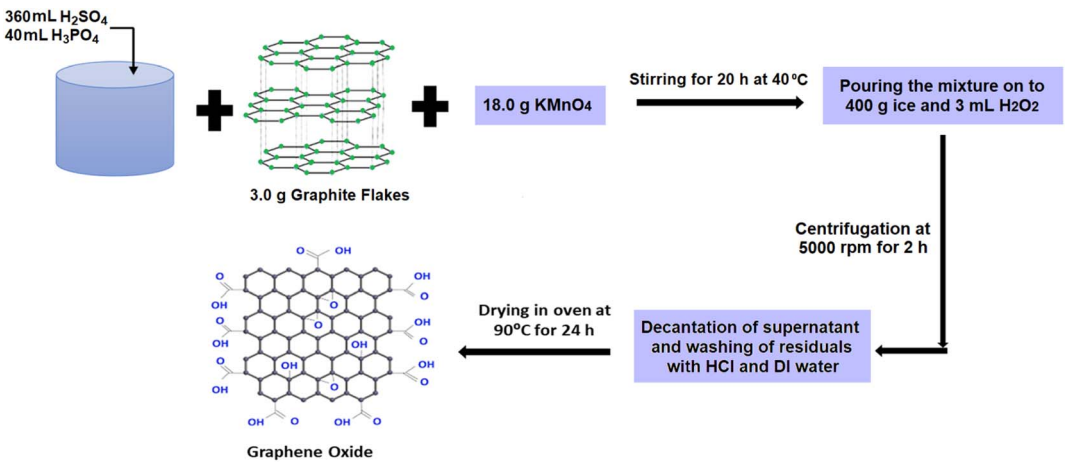


Fig. 1 Preparation of GO by a modified Hummers method.

imaged under an OM, and the underwater oil CA was measured using a contact angle goniometer.

## 3. Results and discussion

GO monolayers possess $sp^2$ hybridized carbon atoms and partly $sp^3$ hybridized carbon atoms having oxygen-containing functional groups. Fig. 2A reveals the FTIR transmittance spectra of the as-prepared GO powder. The broad peak at 3442.31 $cm^{-1}$ can be assigned to the stretching of the O–H bond, which is in the high-frequency area. This reveals the presence of hydroxyl groups bonded onto carbon at several places in the GO molecular structure. The bands at 1722.121 $cm^{-1}$ and 1628.5 $cm^{-1}$ depict C=O and C=C bonds, respectively, which confirms the presence of the carboxylic acid group and aromatic groups. The band at 1395.24 $cm^{-1}$ can be due to the stretching of the C–OH group in water molecules soaked onto GO sheets. Similarly, the bands at 1219.75 $cm^{-1}$ and 1044.56 $cm^{-1}$ can be due to the

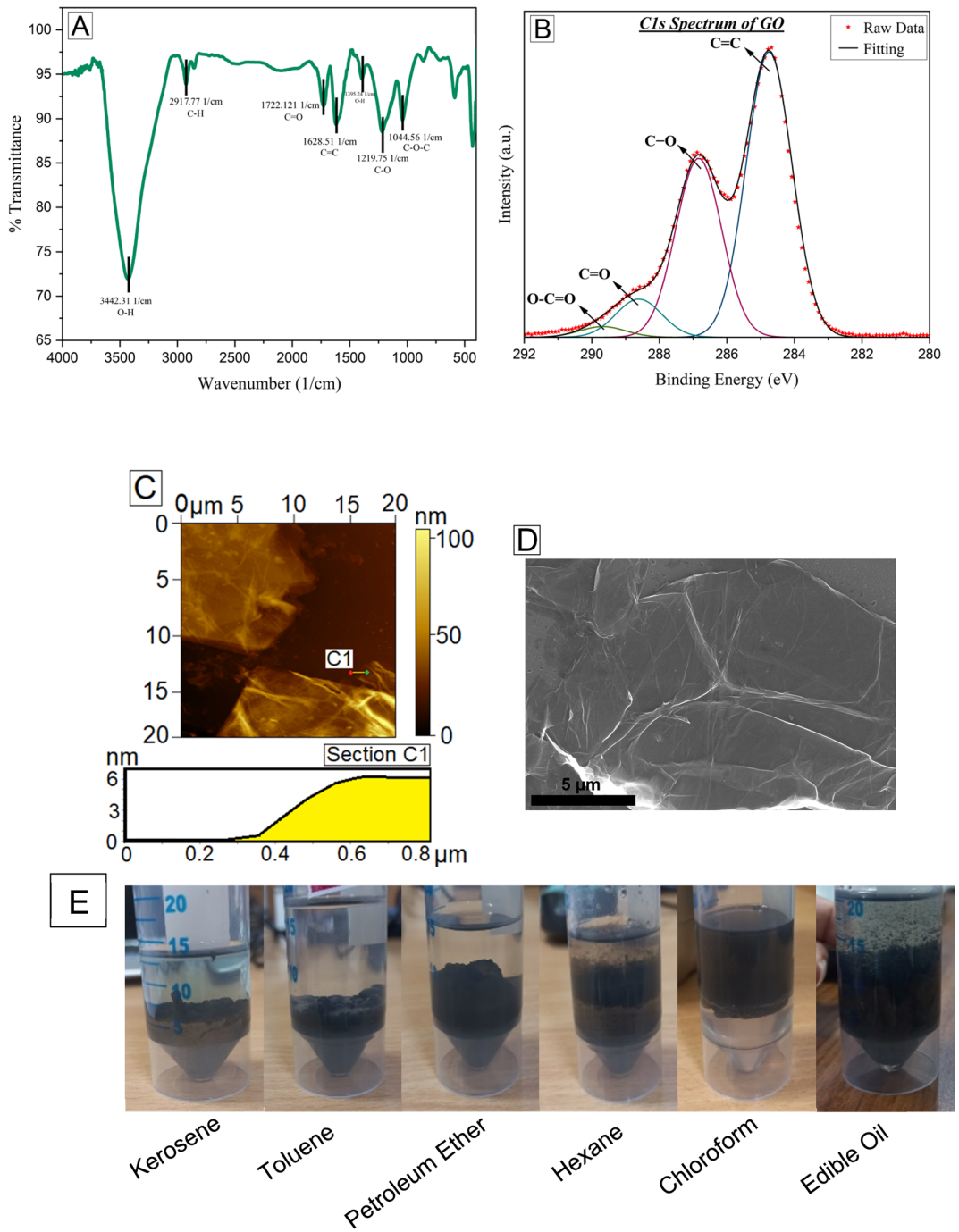


Fig. 2 (A) FTIR spectrum of GO. (B) XPS C 1s spectrum of GO. (C) AFM image of GO sheets coated on a silicon wafer. (D) FESEM image of GO sheets. (E) GO dispersion in water and various nonpolar solvents for testing its hydrophilicity.

stretching of C–O (epoxy) groups. Fig. 2B shows the XPS C 1s spectra of the as-prepared GO powder. After deconvolution, it is distinctly apparent that the C 1s spectrum contains four peaks at 284.78 eV, 286.88 eV, 288.68 eV, and 289.78 eV, which are attributed to the C=C bond (in the aromatic ring), C–O bond (in hydroxyl and epoxy groups), C=O bond (carbonyl group) and O–C=O (carboxyl group) respectively. We can clearly infer from the intensities of the peaks that GO has been oxidized satisfactorily.[33] Fig. 2C and D show the AFM and FESEM images, respectively of the GO sheets on the silicon wafer substrate. Both AFM and FESEM images show the presence of thin sheets along with wrinkle-like structures on the GO surface. This wrinkle formation may have been observed due to the coating and the drying process on the substrate.[36] To check the level of oxidation and hydrophilicity, the GO powder was dispersed in water and mixed with an equal amount of different non-polar solvents with vigorous shaking by hand. The nonpolar solvents used were kerosene, toluene, petroleum ether, hexane, chloroform, and edible sunflower oil, as shown in Fig. 2E. As the dispersion settled, we observed that most of the GO was present in the water phase proving the hydrophilic properties of GO. Some amount of GO was also seen in the interface between water and the non-polar solvents, as GO can also act as an amphiphilic material due to the $sp^2$ conjugated system.[27]

Fig. 3A shows the OM images of the brass mesh (~300 μm pore size) after cleaning and plasma treatment. The initial plasma treatment was done to remove any impurities, increase the surface energy and oxidize the surface for better binding of GO to the mesh. To achieve uniform coverage of GO on the mesh, we dip-coated the mesh with the GO dispersion five times with intermediate drying after each coating. Fig. 3B shows the mesh after applying three coats of GO. After coating five times, we observed that most of the pores in the mesh were covered with a continuous GO film, as seen in Fig. 3C. To open the fully obturate pores, the mesh was subjected to air plasma treatment from one side for 1 min.[28] Plasma treatment leads to strong oxidation and etching of GO from the pores of the mesh while the GO coating on the opposite side of the mesh remains intact. After treatment, we obtained a GO*-coated mesh with all open pores with an average pore size of 202 ± 15 μm, as seen in Fig. 3D. While applying multiple layers of coating helps in ensuring uniform coverage of the mesh with GO, the final plasma treatment can be used to open pores with control of pore size.

The in-air wettability and underwater oleophobicity of the mesh were quantified using contact angle (CA) measurements. The bare mesh showed slight hydrophobicity in the air with a CA of ~92.7° ± 1.6°. The image of a water drop on the brass mesh is shown in Fig. 4A. The GO-coated mesh was hydrophilic with an initial CA of 81.3° ± 2.2° which reduced to 29.0° slowly over 15 min as water permeated through the mesh (Fig. 4B). Upon coating GO following our protocol which includes plasma treatment steps, we observed an initial CA of 74.3° ± 2°. The water drops quickly permeated through the GO*-coated mesh, and the CA reduced to 5.5° within 30 s, and the drop fully disappeared (Fig. 4C). The improved hydrophilic nature of the GO*-coated mesh and open pores obtained after plasma treatment makes water permeate through the membrane very quickly, which is an essential property for high flux underwater oil/water separation application. The underwater oil CA was

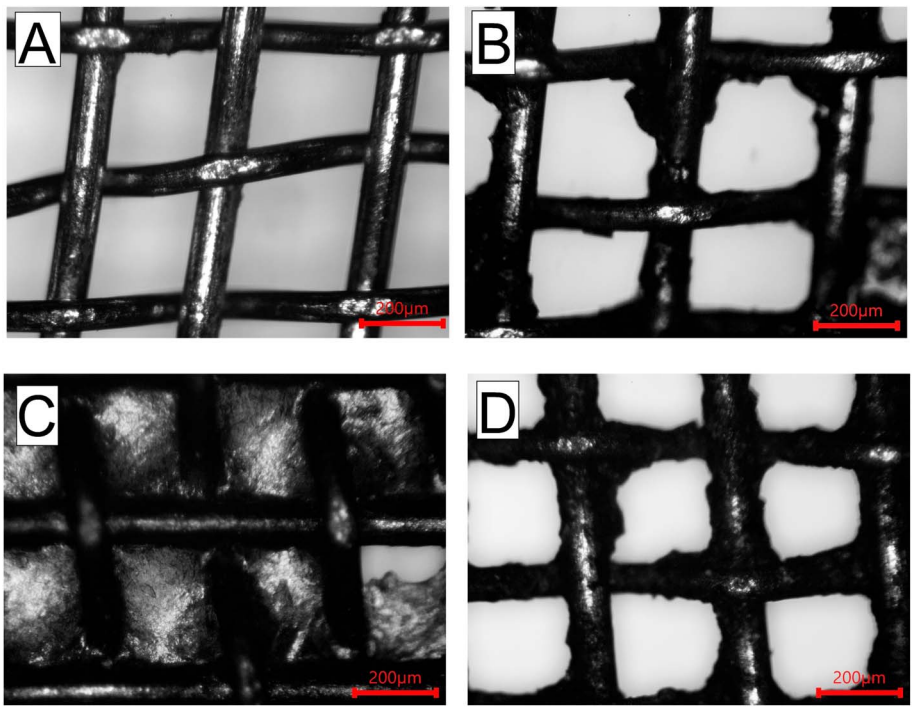


Fig. 3 Optical microscope images of the brass mesh (A) after cleaning and plasma treatment, (B) after dip coating three times with GO, and (C) after dip coating five times with GO, as well as (D) open pores after final plasma treatment. The scale bar represents 200 μm.

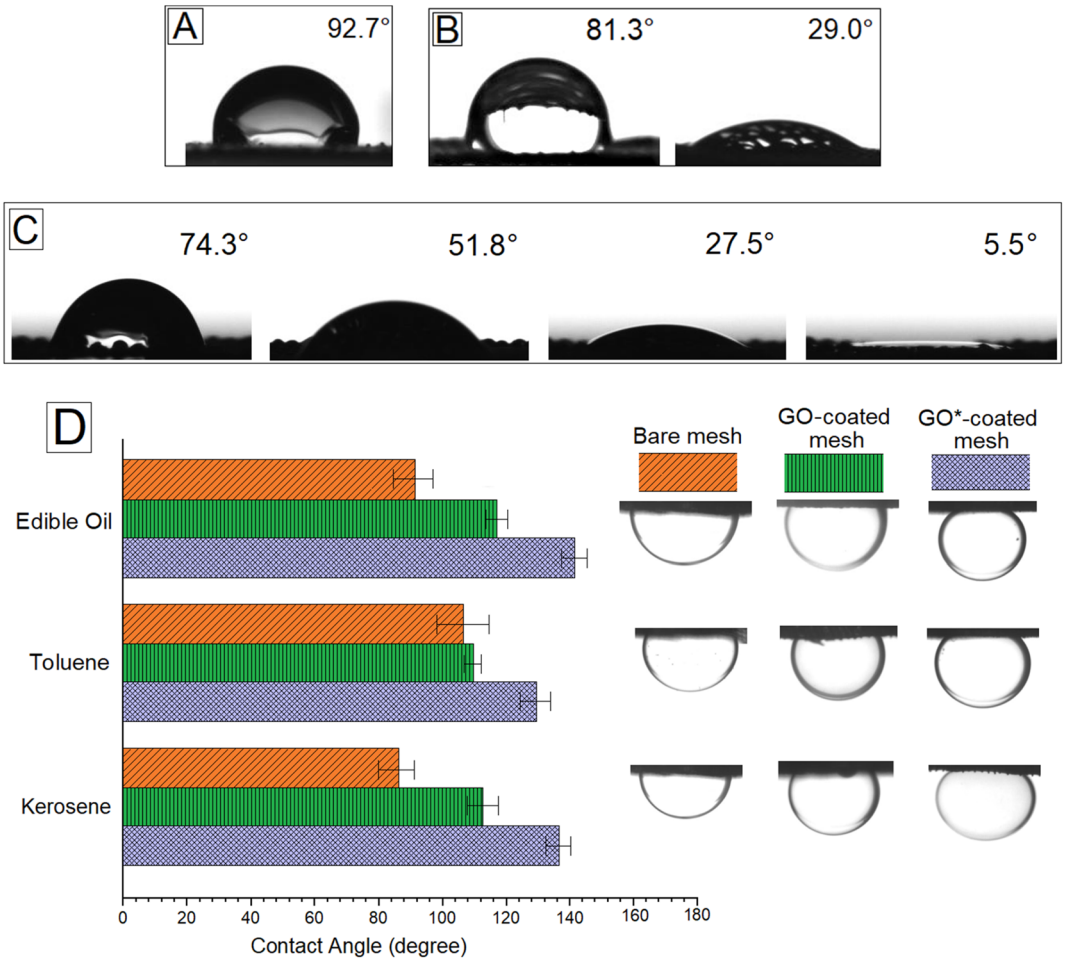


Fig. 4 (A) In-air water CA on an uncoated bare mesh. (B) CA of water on the GO-coated mesh reduced over 15 min from 81.3° to 29.0°. (C) CA of water on the GO*-coated mesh was measured to be 74.3° which reduced as the water permeated immediately through the open pores. (D) Underwater CA of edible oil, toluene, and kerosene on bare mesh, GO-coated mesh, and GO*-coated mesh. Insets show the images of the oil drops.

measured by placing the mesh samples upside down and immersing in water near the top of a water bath. Drops of oil or organic solvent like toluene were created in the water bath and were allowed to deposit on the mesh as the drops moved upwards due to density difference. The CA data and images of oil drops on bare mesh, GO-coated mesh, and GO*-coated mesh are shown in Fig. 4D for edible oil, toluene, and kerosene. The GO*-coated mesh showed a CA of 130° or above for the three oils, whereas the GO-coated mesh showed a CA of above 110° for the three oils. The bare mesh showed CA between 85° and 105°. This is a considerable improvement in oleophobic properties for a coarse mesh with ~300 μm pore size. The reason behind the underwater oleophobicity of the GO*-coated mesh is its super hydrophilicity which is a combined effect of GO coating and plasma treatment. Typically, the liquid CA and wettability on a solid surface in the air are determined using Young's equation.[1] Young's equation can be modified for different settings, including the determination of CA of a liquid on a solid surface immersed in a second liquid.[18] The modified equation can be written as:

$$\cos\theta_3 = \frac{\gamma_{o-a}\cos\theta_1 - \gamma_{w-a}\cos\theta_2}{\gamma_{o-w}} \quad (1)$$

where $\gamma_{o-a}$ is the oil–air interface tension, $\theta_1$ is the CA of oil in the air, $\gamma_{w-a}$ is the water–air interface tension, $\theta_2$ is the CA of water in the air, $\gamma_{o-w}$ is the oil/water interface tension, and $\theta_3$ is the CA of oil in water. We have calculated the values of $\theta_3$ for edible oil and non-polar liquids using in-air CA values (Table S1, ESI†). If we take edible oil as an example, $\gamma_{o-a} = 31.5$ mN m$^{-1}$, $\gamma_{w-a} = 72.8$ mN m$^{-1}$ and $\gamma_{o-w} = 37.04$ mN m$^{-1}$. The CA of edible oil ($\theta_1$) on a GO-coated glass slide in the air was ~10.5° ± 0.6°. The initial CA of water on a glass slide coated once with GO ($\theta_2$) was measured to be 59.8° ± 3°. Therefore, using eqn (1), the CA of edible oil on the glass slide when placed underwater ($\theta_3$) was calculated to be 105.5°. This shows that GO-coated surfaces show oleophobic nature underwater. Eqn (1) also shows that a decrease in the value of $\theta_2$ will lead to an increase in the value of $\theta_3$. Thus, a more hydrophilic surface in air will show better oleophobicity underwater. With our coating process using multiple rounds of dip coating and plasma treatment, we were able to make meshes with significantly lower values of $\theta_2$ (as

shown in Fig. 4B) and achieve superoleophobicity underwater.

The durability of the coating on the mesh is a significant factor in determining the long-term usage of the mesh in applications such as oil/water separation. While a myriad of fabrication techniques have been proposed to date, the foremost challenge with all the techniques is the poor durability against external influences.[4] Many works have reported the stable separation efficiency of the membranes after repeated cycles of oil/water separation tests. Some of the works went one step ahead and tested chemical and thermal stability by using water/oil mixtures containing hot water, acidic water, basic water, or salt.[28,31,37] But only a few groups have studied the long-term durability and chemical stability of the meshes when immersed in a medium for durations up to 24 h.[37] To better understand the long-term durability of the GO*-coated mesh and the stability of the superoleophobic properties of the mesh, we immersed the GO*-coated mesh samples in water, acidic medium, and basic medium continuously for up to 60 days. We took out different samples at intermediate durations, dried them naturally, and imaged and measured the underwater oil CA.

Fig. 5A and B show the GO-coated mesh and GO*-coated mesh immersed in water, respectively. Upon continuous immersion for 10 days, we observed that the GO-coated mesh started leaching out, and the GO flakes dispersed into the water slowly, as seen in Fig. 5A. Under an OM, we can see that the coating is missing from several parts of the mesh, as shown in Fig. 5E. For the GO*-coated mesh samples, we did not see any GO flakes leaching out even after 60 days of continuous immersion (Fig. 5B). This experiment gives preliminary proof that the initial step of plasma treatment has helped in improving the adhesion between GO flakes and the brass mesh. Fig. 5F shows the OM image of the mesh after 60 days of continuous immersion in water. We can see that the mesh is still coated with the GO and looks similar to the GO*-coated mesh shown in Fig. 3D.

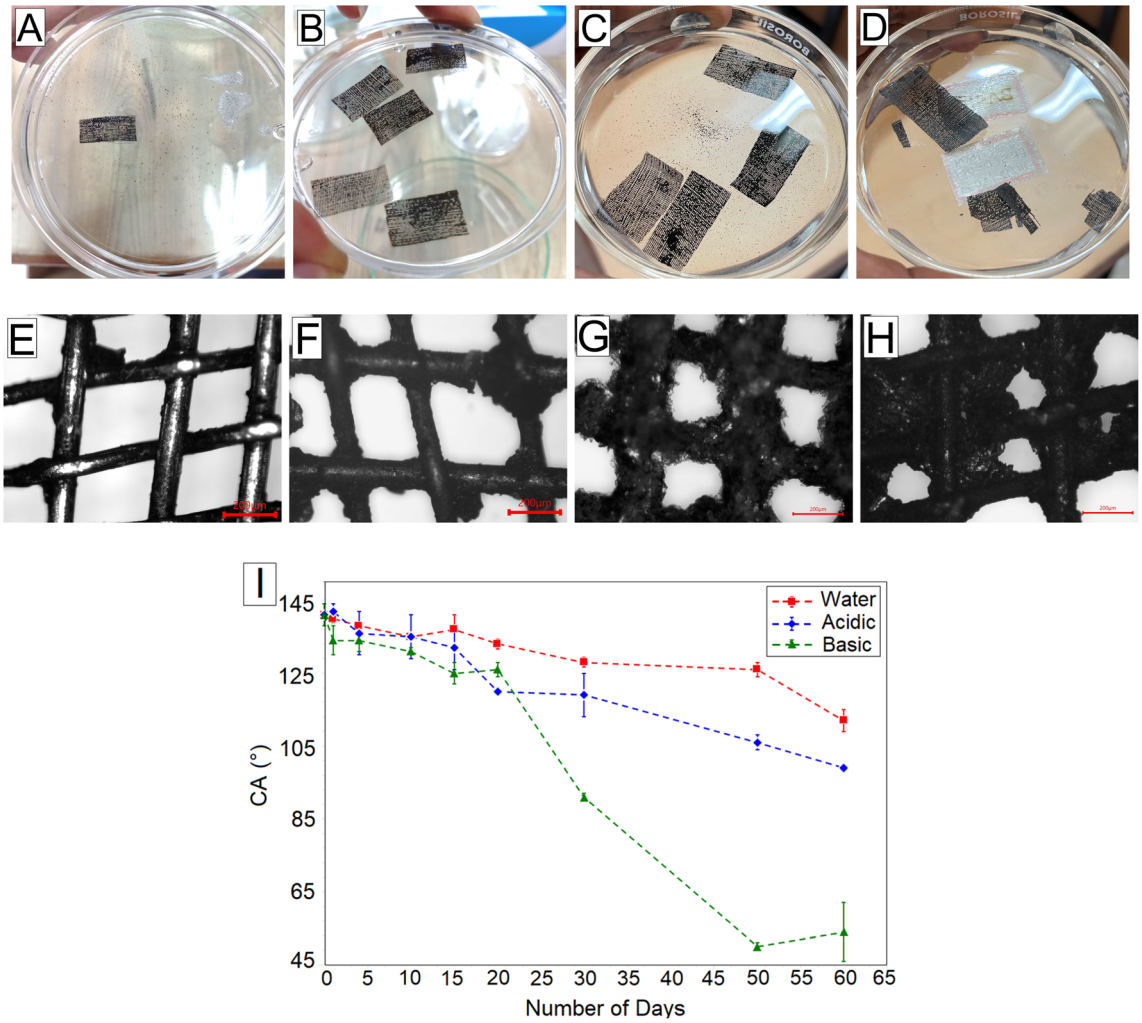


Fig. 5 (A and E) GO-coated mesh immersed in water for 10 days and the corresponding OM image of the mesh after drying. GO*-coated mesh samples immersed continuously for 60 days in (B and F) water, (C and G) acidic medium, and (D and H) basic medium. The scale bar for OM images represents 200 μm. (I) Variation in the underwater edible oil CA when the GO*-coated mesh was immersed in water, acidic medium and basic medium for time durations up to 60 days.

In a low pH medium, it has been reported that the carboxyl groups of the GO sheets become protonated, lose their hydrophilic properties, and form aggregates.[38] When GO*-coated meshes were immersed in an acidic medium, we observed a similar process of gradual formation of aggregates in the medium, which was clearly visible after 60 days of continuous immersion, as seen in Fig. 5C. The formed aggregates may detach from the mesh and remain suspended in the medium. Fig. 5G shows the OM image of the same mesh in which the GO coating around the wire mesh appears to be swollen with pore size $\sim 63 \pm 2$ μm. The swelling can be due to the protonated carboxyl groups of GO in an acidic medium, which can form stable layered aggregates of GO and water.[38,39] In a basic medium, the ionization of the carboxylic groups may cause the dissolution of GO sheets into the medium.[39] While we did not observe any change in the color of the basic medium even after 60 days of continuous immersion, the brass mesh became very brittle and corroded due to dezincification in the high pH medium (Fig. 5D). The dissolution of the GO coating exposed the brass mesh which caused faster corrosion. Fig. 5H shows that the pore size of the mesh in the basic medium has been reduced to $\sim 50 \pm 8$ μm, and a few pores have closed up.

For the GO-coated mesh, after ten days of continuous immersion in water, the underwater edible oil CA reduced from 138.2° to 90.0° (35% reduction). The leaching of GO flakes reduces the oleophobicity, and the edible oil CA was similar to that of the bare mesh. In contrast, for the GO*-coated mesh, the edible oil CA reduced from 141.0° ± 3.0° to 135.0° ± 0.6° (4% reduction) after ten days of continuous immersion in water. Fig. 5I shows the variation in the underwater edible oil CA when the GO*-coated mesh is immersed continuously in water, acidic medium and basic medium for different durations of time up to 60 days. In the neutral medium, the GO*-coated mesh remains significantly oleophobic with an underwater edible oil CA of 112.0° ± 3.0° after 60 days of immersion (20.6% reduction). This shows that the GO*-coated mesh is much more durable than the GO-coated mesh. In an acidic medium, the formation of aggregates and leaching of GO flakes affected the oleophobicity as the edible oil CA dropped to 99° ± 1.0° after 60 days (30% reduction). The basic medium caused maximum degradation of the GO coating as the edible oil CA dropped to 54° ± 8.0° (61.7% reduction). Still, Fig. 5I confirms that all the GO*-coated meshes maintain significant oleophobicity (underwater oil CA > 120°) after 20 days of continuous immersion.

Apart from oil CA, another important physical property for oil/water separation application is the breakthrough pressure, the maximum pressure required to make the liquid permeate through the mesh.[6] For an underwater superoleophobic mesh, the breakthrough pressure, $\Delta P_C^w$, depends on $r_P$ (radius of the mesh pores) and is given as:

$$\Delta P_C^w = -\frac{2\gamma_{o-w}\cos\theta_3}{r_P} \quad (2)$$

For the GO*-coated mesh, the theoretical value of $\Delta P_C^w$ was calculated to be 621.7 Pa, for $r_P = 101$ μm. Upon continuous immersion in water, acidic medium and basic medium for 60 days, the theoretical $\Delta P_C^w$ reduced to 272.4 Pa, 198.6 Pa and −940.5 Pa respectively. This shows that along with degradation of superoleophobicity, the maximum pressure that the mesh can withstand also reduces. A negative value of $\Delta P_C^w$ in the basic medium indicates that the oil will spontaneously penetrate through the mesh without any external force and the mesh cannot be used for oil/water separation. Using $\Delta P_C^w = h_{max}\rho g$ ($\rho$ is the density of edible oil, $g$ is the acceleration due to gravity, and $h_{max}$ is the maximum height of the edible oil column that the mesh can support), the theoretical value of $h_{max}$ over a fresh GO*-coated mesh was ∼6.9 cm. We also measured the stability of a 10 cm oil column over the GO*-coated mesh and found that the oil column remains stable over the mesh even after 30 min of observation. This shows that the experimental value of the breakthrough pressure for the mesh was ∼900.4 Pa.

## 4. Conclusion

In this work, we show that intermediate steps of air plasma treatment during the coating of GO on a wire mesh significantly improve its hydrophilic and underwater oleophobic properties towards different types of low surface tension liquids (edible oil, toluene, kerosene). We used a wire mesh with a large pore size (300 μm) and multiple GO dip coating steps followed by plasma treatment to open up the fully obturate pores and control pore size to obtain a GO*-coated mesh. The underwater oil CA significantly increased by at least 30% for different liquids as compared to bare mesh. In addition to this, we tested the long-term durability of the GO*-coated mesh in acidic, basic and neutral media. The GO*-coated mesh performs much better than the GO-coated mesh (without plasma treatment) when immersed continuously underwater for 60 days. While the GO-coated mesh lost underwater oleophobicity in 10 days and leaching of GO flakes was observed, the GO*-coated mesh maintained high oil CA even after 60 days of continuous immersion. We can infer that plasma treatment not only helps unclog obturate pores, but also improves the binding of the GO coating to the mesh. In acidic and basic media, the protonation or ionization of GO leads to gradual degradation of the coating. The maximum degradation was observed in the basic medium as the underwater oil CA reduced by 61.7%. This work highlights that while methods such as air plasma treatment can improve the underwater oleophobicity of the GO-coated mesh, it is also extremely important to study the long-term durability of these coatings upon continuous immersion in water and other media before proposing them as good oil/water separation membranes.

## Author contributions

P. S. and M. D. contributed equally to the work. N. B. conceived the idea of this work. P. S., M. D. and N. B. planned the experiments. M. D. carried out the initial lab experiments, and P. S. performed the durability studies. All the authors contributed to the writing of the manuscript.

## Conflicts of interest

The authors declare no conflict of interest.

## Acknowledgements

N. B. acknowledges the financial support from the Department of Science & Technology (DST), New Delhi, in the form of a DST INSPIRE Faculty Award [DST/INSPIRE/04/2016/002396] and an Additional Competitive Research Grant (BITS Project ID 919) from BITS Pilani.

## References

1 V. M. Naik, R. Mukherjee, A. Majumder and A. Sharma, Super functional materials: creation and control of wettability, adhesion and optical effects by meso-texturing of surfaces, *Curr. Trends Sci.–Platin. Jubil. Spl*, 2009, 129–148.
2 R. Hensel, C. Neinhuis and C. Werner, The springtail cuticle as a blueprint for omniphobic surfaces, *Chem. Soc. Rev.*, 2016, **45**, 323–341.
3 X. Liu, J. Zhou, Z. Xue, J. Gao, J. Meng, S. Wang and L. Jiang, Clam's shell inspired high-energy inorganic coatings with underwater low adhesive superoleophobicity, *Adv. Mater.*, 2012, **24**, 3401–3405.
4 B. Wang, W. Liang, Z. Guo and W. Liu, Biomimetic super-lyophobic and super-lyophilic materials applied for oil/water separation: A new strategy beyond nature, *Chem. Soc. Rev.*, 2015, **44**, 336–361.
5 R. K. Gupta, G. J. Dunderdale, M. W. England and A. Hozumi, Oil/water separation techniques: a review of recent progresses and future directions, *J. Mater. Chem. A*, 2017, **5**, 16025–16058.
6 C. Chen, D. Wang, A. Mahmood, S. Chen and J. Wang, Separation mechanism and construction of surfaces with special wettability for oil/water separation, *ACS Appl. Mater. Interfaces*, 2019, **11**, 11006–11027.
7 Y. Zhu, D. Wang, L. Jiang and J. Jin, Recent progress in developing advanced membranes for emulsified oil/water separation, *NPG Asia Mater.*, 2014, **6**, e101.
8 N. P. Ventikos, E. Vergetis, H. N. Psaraftis and G. Triantafyllou, A high-level synthesis of oil spill response equipment and countermeasures, *J. Hazard. Mater.*, 2004, **107**, 51–58.
9 A. A. Al-Shamrani, A. James and H. Xiao, Destabilisation of oil–water emulsions and separation by dissolved air flotation, *Water Res.*, 2002, **36**, 1503–1512.
10 E. R. Binner, J. P. Robinson and S. W. Kingman, Separation of oil/water emulsions in continuous flow using microwave heating, *Energy Fuels*, 2013, **27**, 3173–3178.
11 P. Calcagnile, D. Fragouli, I. S. Bayer, G. C. Anyfantis, L. Martiradonna, P. D. Cozzoli, R. Cingolani and A. Athanassiou, Magnetically driven floating foams for the removal of oil contaminants from water, *ACS Nano*, 2012, **6**, 5413–5419.
12 D. D. Nguyen, T. Nyan-Hwa, L. San-Boh and K. Wen-Shyong, Superhydrophobic and superoleophilic properties of graphene-based sponges fabricated using a facile dip coating method, *Energy Environ. Sci.*, 2012, **5**, 7908–7912.
13 J. Zhang and S. Seeger, Polyester materials with superwetting silicone nanofilaments for oil/water separation and selective oil absorption, *Adv. Funct. Mater.*, 2011, **21**, 4699–4704.
14 G. Wen, Z. Guo and W. liu, Biomimetic polymeric superhydrophobic surfaces and nanostructures: From fabrication to applications, *Nanoscale*, 2017, **9**, 3338–3366.
15 J. Yong, F. Chen, Q. Yang, J. Huoa and X. Houa, Superoleophobic surfaces, *Chem. Soc. Rev.*, 2017, **46**, 4168–4217.
16 A. R. Bielinski, M. Boban, Y. He, E. Kazyak, D. H. Lee, C. Wang, A. Tuteja and N. P. Dasgupta, Rational design of hyperbranched nanowire systems for tunable superomniphobic surfaces enabled by atomic layer deposition, *ACS Nano*, 2017, **11**, 478–489.
17 L. Feng, Z. Zhang, Z. Mai, Y. Ma, B. Liu, L. Jiang and D. Zhu, A super-hydrophobic and super-oleophilic coating mesh film for the separation of oil and water, *Angew. Chem., Int. Ed.*, 2004, **43**, 2012–2014.
18 M. Liu, S. Wang, Z. Wei, Y. Song and L. Jiang, Bioinspired design of a superoleophobic and low adhesive water/solid interface, *Adv. Mater.*, 2009, **21**, 665–669.
19 Z. Xue, S. Wang, L. Lin, L. Chen, M. Liu, L. Feng and L. Jiang, 19, A novel superhydrophilic and underwater superoleophobic hydrogel coated mesh for oil/water separation, *Adv. Mater.*, 2011, **3**, 4270–4273.
20 M. Liu, J. Li, L. Shi and Z. Guo, Stable underwater superoleophobic conductive polymer coated meshes for high-efficiency oil-water separation, *RSC Adv.*, 2015, **5**, 33077–33082.
21 L. Feng, Z. Zhang, Z. Mai, Y. Ma, B. Liu, L. Jiang and D. Zhu, A super-hydrophobic and super-oleophilic coating mesh film for the separation of oil and water, *Angew. Chem., Int. Ed.*, 2004, **43**, 2012–2014.
22 A. K. Kota, G. Kwon, W. Choi, J. M. Mabry and A. Tuteja, Hygro-responsive membranes for effective oil–water separation, *Nat. Commun.*, 2012, **3**, 1025.
23 F. Li, Z. Wang, S. Huang, Y. Pan and X. Zhao, Flexible, Durable, and unconditioned superoleophobic/superhydrophilic surfaces for controllable transport and oil–water separation, *Adv. Funct. Mater.*, 2018, **28**, 1706867.
24 F. Zhang, W. Bin Zhang, Z. Shi, D. Wang, J. Jin and L. Jiang, Nanowire-haired inorganic membranes with superhydrophilicity and underwater ultralow adhesive superoleophobicity for high-efficiency oil/water separation, *Adv. Mater.*, 2013, **25**, 4192–4198.
25 L. Liu, C. Chen, S. Yang, H. Xie, M. G. Gong and X. Xu, Fabrication of superhydrophilic-underwater superoleophobic inorganic anti-corrosive membranes for high-efficiency oil/water separation, *Phys. Chem. Chem. Phys.*, 2015, **18**, 1317–1325.
26 Z. Lian, J. Xu, Z. Wang, Z. Yu, Z. Weng and H. Yu, Nanosecond laser-induced underwater superoleophobic and underoil superhydrophobic mesh for oil/water separation, *Langmuir*, 2018, **34**, 2981–2988.

27 Y. Dong, J. Li, L. Shi, X. Wang, Z. Guo and W. Liua, Underwater superoleophobic graphene oxide coated meshes for the separation of oil and water, *Chem. Commun.*, 2014, **50**, 5586–5589.
28 L. Yu-Qing, Z. Yong-Lai, F. Xiu-Yan and S. Hong-Bo, Bioinspired underwater superoleophobic membrane based on a graphene oxide coated wire mesh for efficient oil/water separation, *ACS Appl. Mater. Interfaces*, 2015, **7**, 20930–20936.
29 M. Fathizadeh, W. L. Xu, F. Zhou, Y. Yoon and M. Yu, Graphene oxide: a novel 2-dimensional material in membrane separation for water purification, *Adv. Mater. Interfaces*, 2017, **4**, 1600918.
30 T. Huang, L. Zhang, H. Chena and C. Gaoa, Sol–gel fabrication of a non-laminated graphene oxide membrane for oil/water separation, *J. Mater. Chem. A*, 2015, **3**, 19517–19524.
31 C. Chen and B. Chen, Graphene oxide coated meshes with stable underwater superoleophobicity and anti-oil-fouling property for highly efficient oil/water separation, *Sci. Total Environ.*, 2019, **696**, 133777.
32 S. M. Varughese and N. Bhandaru, Durability of submerged hydrophobic surfaces, *Soft Matter*, 2020, **16**, 1692–1701.
33 D. C. Marcano, D. V. Kosynkin, J. M. Berlin, A. Sinitskii, Z. Sun, A. Slesarev, L. B. Alemany, W. Lu and J. M. Tour, Improved synthesis of graphene oxide, *ACS Nano*, 2010, **4**, 4806–4814.
34 G. Santamaría-Juárez, E. Gómez-Barojas, E. Quiroga-González, E. Sánchez-Mora, M. Quintana-Ruiz and J. D. Santamaría-Juárez, Safer modified Hummers' method for the synthesis of graphene oxide with high quality and high yield, *Mater. Res. Express*, 2020, **6**, 125631.
35 N. Bhandaru, G. Kaur, A. Panjil and S. Verma, Spin coating mediated morphology modulation in self assembly of peptides, *Nanoscale*, 2021, **13**, 8884–8892.
36 B. Lian, S. De Luca, Y. You, S. Alwarappan, M. Yoshimura, V. Sahajwalla, S. C. Smith, G. Lesliea and R. K. Joshi, Extraordinary water adsorption characteristics of graphene oxide, *Chem. Sci.*, 2018, **9**, 5106–5111.
37 J. Wang, J. Wu and F. Han, Eco-friendly and scratch-resistant hybrid coating on mesh for gravity-driven oil/water separation, *J. Cleaner Prod.*, 2019, **241**, 118369.
38 F. Yu, A. C. Stoot, P. Bøggild and L. Camilli, Failure of multi-layer graphene coatings in acidic media, *RSC Adv.*, 2016, **6**, 21497–21502.
39 S. Chih-Jen, S. Lin, R. Sharma, M. S. Strano and D. Blankschtein, Understanding the pH-dependent behavior of graphene oxide aqueous solutions: a comparative experimental and molecular dynamics simulation study, *Langmuir*, 2012, **28**, 235–241.